

**INTEGRATION SURFACE IN APERTURE FIELD INTEGRATION METHOD FOR EQUIVALENCE TO PHYSICAL OPTICS**

Masayuki Oodo\*, Hidetaka Nishikoori and Makoto Ando  
 Dept. of Electrical & Electronic Engineering, Tokyo Institute of Technology  
 2-12-1, O-okayama, Meguro-ku, Tokyo 152, Japan

**1. Introduction**

The equivalence of physical optics (PO) and aperture field integration method (AFIM) in the full 360° angular direction of reflector antennas is discussed from two viewpoints in AFIM; (1)one is how to select the integration surface and (2)the other is how to approximate the equivalent currents on the integration surface. For smooth parabolic reflectors, it was already shown analytically[1][2] and numerically[2]-[5] that AFIM predicts the full angular patterns as accurately as PO even in very low frequency range provided the following conditions in AFIM are satisfied.

- (1) The integration surface perfectly caps the reflector such as  $S_a$  in Fig.1[1][2].
- (2) The equivalent electric and magnetic currents  $I(q_a)$  and  $M(q_a)$  at the point  $q_a$  on  $S_a$  are defined by not only the geometrical optics (GO) reflected electric and magnetic fields  $E^r(q_a)$  and  $H^r(q_a)$  by the parabolic reflector but also the incident fields  $E^i(q_a)$  and  $H^i(q_a)$  from the feed as is shown in Fig.2[2][4][5]. Namely

$$I(q_a) = \hat{n}(q_a) \times (H^i(q_a) + H^r(q_a)), \quad M(q_a) = (E^i(q_a) + E^r(q_a)) \times \hat{n}(q_a) \quad (1)$$

where  $\hat{n}(q_a)$  denotes the outward unit vector at  $q_a$  which is normal to the integration surface  $S_a$  and

$$E^r(q_a) = E^r(q_s)e^{-jk|q_a - q_s|}, \quad H^r(q_a) = \hat{s} \times E^r(q_a)/Z_0 \quad (2)$$

$\hat{s}$  and  $Z_0$  denote the unit vector oriented to the boresight direction and the wave impedance of the free space, respectively.  $E^r(q_s)$  denotes the reflected field at  $q_s$  which is the reflection point on the reflector. The direction of all the reflected rays is parallel to the main beam direction.

In this paper, how to select the integration surface in AFIM for polyhedron approximated reflectors is discussed[6][7]. The necessary conditions of the integration surface for the equivalence to PO are shown. One example of the integration surface which satisfies the necessary conditions is proposed and the equivalence of PO and AFIM using that correct integration surface is shown by a 3-D numerical calculation.

**2. Integration Surface in AFIM for Polyhedron Approximated Reflectors**

How to select the integration surface in AFIM for a polyhedron approximated reflector, which is composed of some conducting plates, is discussed. Figure 3 shows the geometry of the reflected rays by one plate  $P_m$ . The reflected fields are calculated by assuming the image sources( $I_m$ 's) of the feed with respect to the plates( $P_m$ 's). The direction of all the reflected rays is not always parallel to the boresight direction. For such cases, a simple aperture of the reflector is not enough as the integration surface[6][7], since the ray spreading effects can not be evaluated accurately. One integration surface should be assigned for one reflecting plate. For example, integration surface  $S_m$  ( $A_m$ - $B_m$ - $C_m$ - $D_m$ ) in Fig.4 is assigned for the plate  $P_m$ [7]. Each integration surface  $S_m$  should cap the plate  $P_m$  and  $S_m$  should be chosen within the illuminated region of the reflected fields by the

plate  $P_m$ . Equivalent currents on  $S_m$  are defined by the reflected fields by the plate  $P_m$  and the incident fields from the feed.

### **3. Numerical Results and Discussions**

The effects of the integration surface in AFIM are numerically demonstrated. Figure 5 shows the 3-D calculation model. The reflector is composed of six triangular conducting plates ( $P_1$ - $P_6$ ). The aperture diameter is  $3\lambda$ . The feed source is a small dipole oriented to the  $x$ -axis and is located at  $(x, y, z)=(0,0,6\lambda)$ .

Two kinds of AFIM (AFIM① and AFIM②) are tested for this model. In AFIM①, a simple hexagonal aperture  $S_a$  shown in Fig.6 is used as the integration surface. The equivalent currents on  $S_a$  are defined by the reflected fields by six image sources and the incident field from the feed. The reflected field component are overlapped near the central area of  $S_a$ .

While in AFIM②, the integration surface satisfying the necessary conditions mentioned in sec.2 is used. Integration surface is assigned for each plate. Each integration surface covers each plate perfectly and each surface is within the illuminated region of the reflected fields by the corresponding plate. Figure 7 shows the integration surface for the plate  $P_1$ . Plate  $P_1$  is capped by three triangular integration surfaces ( $S_1^T$  and two  $S_1^S$ 's). All those surfaces are within the illuminated region of the reflected fields by the plate  $P_1$ . The equivalent currents on those integration surfaces are defined by the reflected fields by the plate  $P_1$  and the incident fields from the feed. In the same manner, the integration surfaces for the other plates ( $P_2$ - $P_6$ ) are chosen and the equivalent currents are defined. In AFIM②, the incident components of the equivalent currents on the surfaces( $S_{1-6}^S$ ) normal to the aperture do not give any effects to the radiation patterns because of the cancellation.

Fig.8 shows the total field patterns in  $x$ - $z$  plane calculated by PO and two kinds of AFIM. AFIM② using a correct integration surface predicts the pattern identical to that by PO. While the discrepancy is observed between PO and AFIM① especially in the main beam direction. These results show the significance of choosing the correct integration surface. In the backward region, the pattern by AFIM① does not deviate so much from the result by PO. This is due to the fact that the fields in the backward region are mainly produced by the equivalent currents defined by the incident fields.

### **4. Conclusion**

How to choose the integration surface in AFIM for polyhedron approximated reflectors was discussed. The necessary conditions of the integration surface for equivalence to PO was shown. One integration surface should be assigned for one reflecting plate. Each integration surface should cap the plate and it should be chosen within the illuminated region of the reflected fields by the corresponding plate. Equivalent currents on each integration surface should be defined by the reflected fields by the corresponding plate and the incident fields from the feed. The equivalence of PO and AFIM using the above correct integration surface was shown by a 3-D numerical calculation.

### **References**

- [1] A.D.Yaghjian, "Equivalence of surface current and aperture field integrations for reflector antennas", *IEEE Trans.*, AP-32, pp.1355-1358 (1984)
- [2] M.Oodo and M.Ando, "Equivalence of physical optics and aperture field integration method (AFIM) -Effects of the integration region in AFIM", (in Japanese), EMT-94-48, pp.57-66 (Oct. 1994)

- [3] H.Matsuura and K.Hongo, "Comparison of induced current and aperture field integrations for an offset parabolic reflector", *IEEE Trans.*, AP-35, pp.101-105 (1987)
- [4] M.Oodo and M.Ando, "Equivalence of physical optics and aperture field integration method in the full pattern analysis", *IEEE AP-S Int. Symp.*, Seattle, pp.66-69 (June, 1994)
- [5] M.Oodo and M.Ando, "Equivalence of physical optics and aperture field integration method in the full pattern analysis -effects of integration surface", *IEEE AP-S Int. Symp.*, Newport Beach, pp.889-892 (June, 1995)
- [6] E.Hanayama and T.Takano, "Analysis of polyhedron approximated reflector antennas", Proceedings of ISAP '92, Sapporo, Japan (1992)
- [7] M.Oodo and M.Ando, "Equivalence of physical optics and aperture field integration method for a polyhedron approximate reflector antenna" (in Japanese), *EMT-95-123*, pp.121-129 (Dec. 1995)

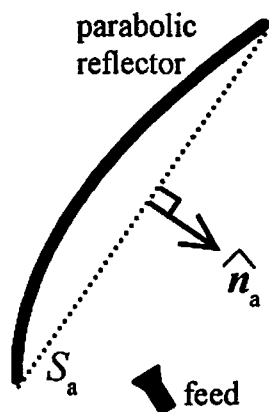


Fig.1 Integration surface  $S_a$  in AFIM for parabolic reflector

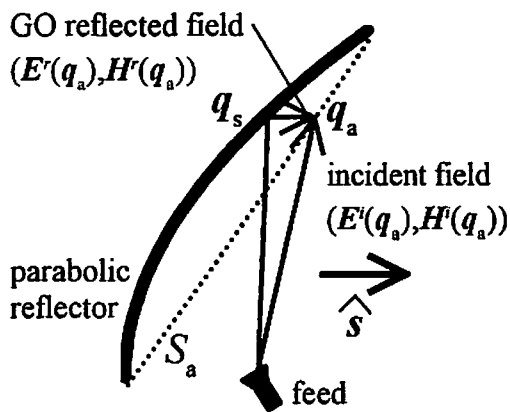


Fig.2 Equivalent currents at  $q_a$  on  $S_a$

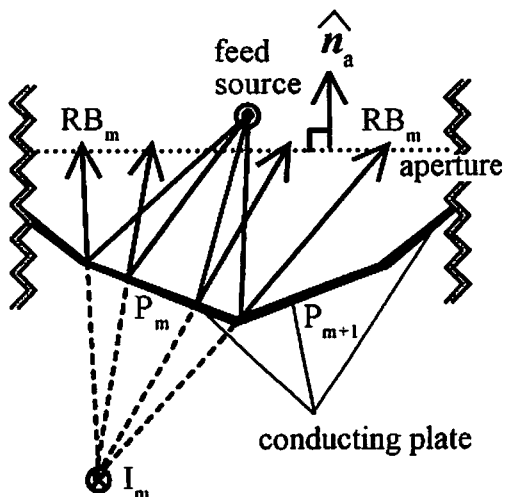


Fig.3 Geometry of the reflected rays by the plate  $P_m$

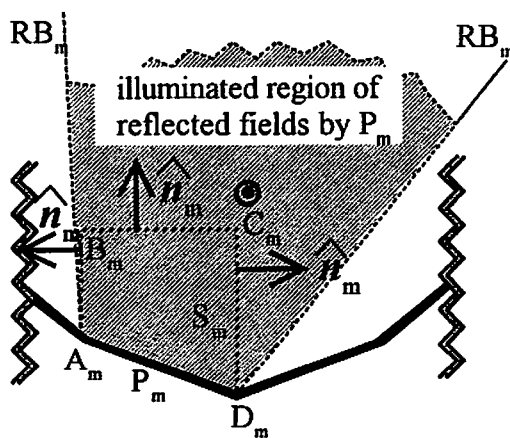


Fig.4 Integration surface  $S_m$  ( $A_m$ - $B_m$ - $C_m$ - $D_m$ ) for the plate  $P_m$

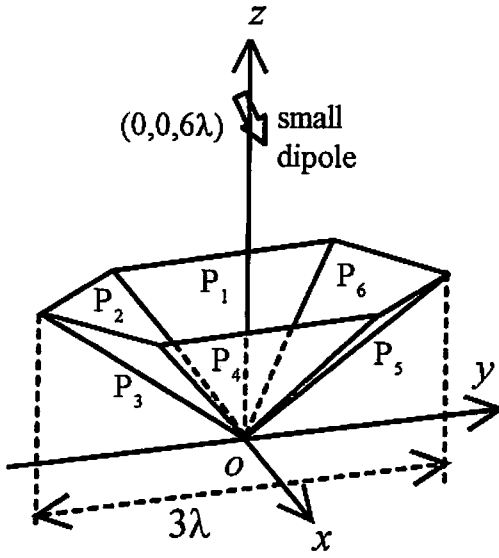


Fig.5 Calculation model composed of six triangular conducting plates( $P_1$ - $P_6$ )

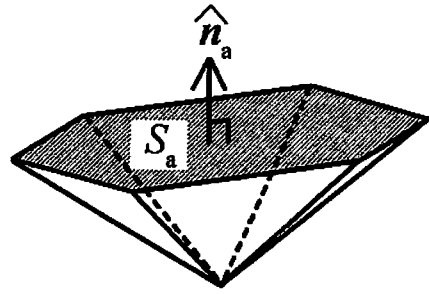


Fig.6 Integration surface  $S_a$

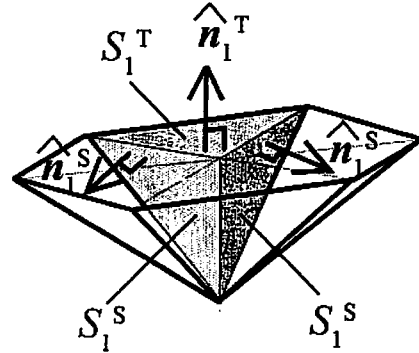


Fig.7 Integration surfaces  $S_1^T$  and  $S_1^S$  for the plate  $P_1$

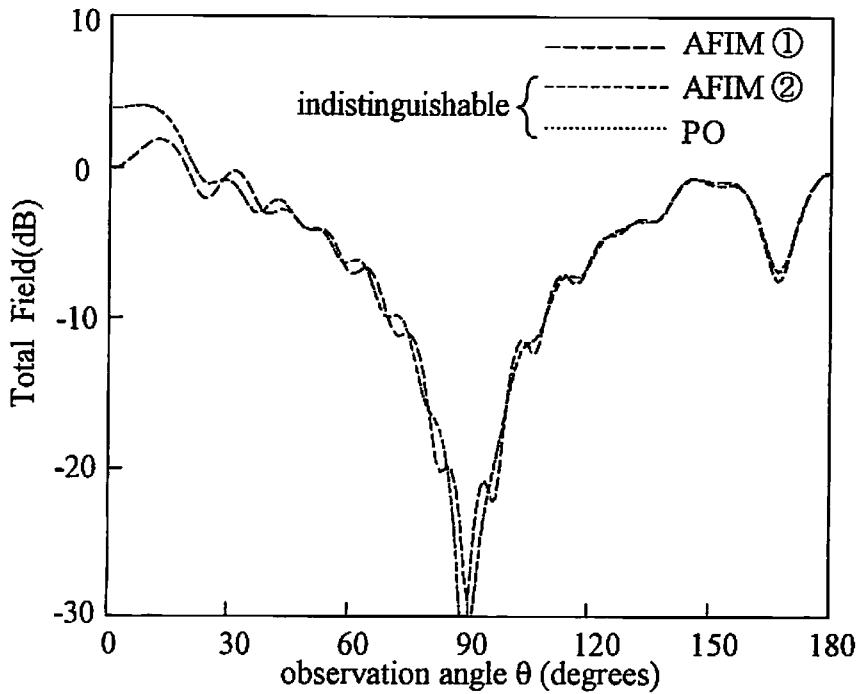


Fig.8 Total field radiation pattern in  $x$ - $z$  plane calculated by PO and two kinds of AFIM